

Specifics in numerical modeling of flow past a square-cylinder

Angel Terziev

Specifics in numerical modeling of flow past a square-cylinder: In paper are discussed issues related numerical modeling of the flow over immersed bodies. Special attention is paid to the choice of appropriate turbulent model for the modeling of fluid flow. Different turbulent models have been tested during the numerical solution procedure as the results have been compared with experimental data. Several conclusions were made based on the obtained by the numerical solution results.

Key words: Turbulence modeling, numerical study, flow past immersed bodies, square cylinder.

INTRODUCTION

The flows around bluff bodies are an area of a great interest for the last three decades. The examples of such kind of flows are flow around buildings in a big cities, distribution of pollutants in the atmosphere and etc. Those types of flows are generally unsteady that additionally complicates their numerical modeling. According to their size the open flows are classified as shown in Figure 1 a-c.

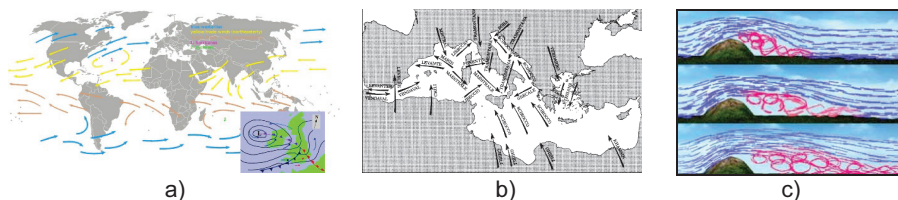


Figure 1. a) Global flow; b) Medium-scale flow; c- small size flow

Generally, the open flows around buildings are turbulent as the generated eddies past the buildings are different in scale. Concerning the scale size, the specifics of large and small size eddies are described in the table below.

Table 1. Specifics in large- and small-size eddies

Large scale eddies	Small scale eddies
Depends on boundary conditions and the geometry	Are generated after decaying of large-scale eddies
Non-homogeny and anisotropic	They are universal
Long-life decay and high energy level	Random
Diffusive	Homogeny and isotropic
Difficult for modeling	Dissipative
Non universal methods available for modeling	Universal models for modeling

The proper selection of a turbulent model is a crucial point in the numerical modeling process.

MATHEMATICAL MODELING. TURBULENCE MODELING

Overview of the experimental studies in the area

Subject of current study is modeling of flow past square-cylinder. There exist two as

well as three-dimensional computations on the flow past a square cylinder. The two-dimensional calculations are not so appropriate at higher Reynolds numbers. Those must be computed using the unsteady three-dimensional Navier-Stokes equations on fine grids. Engineering applications have, however, been computed at high Reynolds number in two-dimensions using various eddy viscosity models of turbulence. Recently the eddy distribution past bluff body flows are presently being computed using large eddy simulation (LES) [1].

Okajima [2, 3] carried out an experimental study of flow past a square cylinder as well as a rectangular cylinder for a wide range of Reynolds numbers, namely $70 \div 2 \cdot 10^4$. The conclusion of the study is that the variation in Strouhal number is the non-dimensional vortex-shedding frequency, with Reynolds numbers. These experiments have shown that there is an abrupt change in Strouhal number when the aspect ratio of the cylinder is reduced to the range 2-3. Durao [4] have conducted laser Doppler velocimetry (LDV) measurements for a flow past a square cylinder in a water tunnel at a Reynolds number of 14 000. They have separated the periodic and random components of velocity fluctuations. These measurements show that the kinetic energy associated with the random components is about 40% of the total. Lyn et al. [5] have reported an LDV study of turbulent flow past a square cylinder with emphasis on the ensemble-averaged characteristics of the flow behavior. The Reynolds number considered in their study was 21 400. The experiments were carried out in a closed and constant head water tunnel. Their results showed a relationship between the flow topology and the turbulence distribution. In addition the differences in length and velocity scales and vortex celerities between the flow around a square cylinder and the more frequently studied flow around a circular cylinder are discussed. The base region is examined in more detail than in previous studies, and vorticity saddles, zero-vorticity points, and streamline saddles are observed to differ in importance at different stages of the shedding process.

Modeling methods classification

Below is presented the classification of different turbulent models applicable for modeling of a turbulent flow passed immersed bodies.

- RANS – stochastic turbulent model (Reynolds averaged Navier – Stokes equations) – used for modeling of the entire turbulent region;
- LES (Large eddy simulation) – for calculation of the large scale eddies. It is a compromise between RANS and DNS;
- DNS (Direct numerical simulation) – calculation of the entire spectrum eddies.

In Figure 2 is presented the relation between degree of modeling and calculation time.

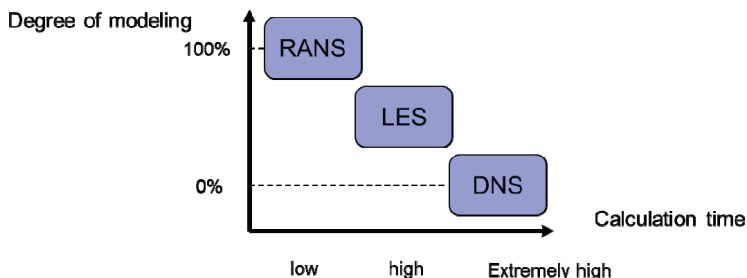
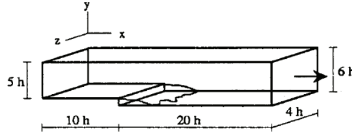


Figure 2. Relation of degree of modeling to calculation time

Limitations of DNS model are presented in table 2.

Table 2. Calculation time of DNS method



DNS	Le/Moin	Hochrechnung		
Re	5100	10 ⁴	10 ⁵	10 ⁶
Gitterpunkte N_G	$9.4 \cdot 10^6$	$42.9 \cdot 10^6$	$7.6 \cdot 10^9$	$1.3 \cdot 10^{12}$
Rechenzeit	1100 h	7000 h	$3.9 \cdot 10^6$ h	$2.2 \cdot 10^9$ h
Cray Y-MP	≈ 46 Tage	≈ 292 Tage	≈ 450 Jahre	253000 Jahre

Turbulence modeling

From a fundamental standpoint, all the currently used two-equation models suffer from lack of an underlying exact transport equation, which can serve as a guide for the model development on a term by term basis. The reason for this deficiency lies in the fact that the exact equation for ϵ does not describe the large scales, but the dissipative scales. The goal of a two-equation model is however the modeling of the influence of the large scale motions on the mean flow. Due to the lack of an exact equation, the dissipation rate (ϵ) – and the specific dissipation (ω) – equations are modeled in analogy with the equation for the turbulent kinetic energy, k , using purely heuristic arguments. A more consistent approach for formulating a scale-equation has been developed by Rotta [6]. Instead of using purely heuristic and dimensional arguments, Rotta formulated an exact transport equation for turbulent kinetic energy times length scale, k_L . Rotta’s equation represents the large scales of turbulence and can therefore serve as a basis for term-by-term modeling. The transport equations for the SAS-SST model which is implemented in ANSYS FLUENT are based on transforming Rotta’s approach k - ω (SST) and defined as:

$$\frac{\partial pk}{\partial t} + \frac{\partial}{\partial x_i} (p u_i k) = G_k - \rho c_\mu k \omega + \frac{\partial}{\partial x_i} \left[\left(\mu + \frac{\mu_t}{\sigma_k} \right) \frac{\partial k}{\partial x_j} \right] \quad (1)$$

$$\frac{\partial p \omega}{\partial t} + \frac{\partial}{\partial x_i} (\rho u_i \omega) = a \frac{\omega}{k} G_k - \rho \beta \omega^2 + Q_{SAS} + \frac{\partial}{\partial x_i} \left[\left(\mu + \frac{\mu_t}{\sigma_\omega} \right) \frac{\partial \omega}{\partial x_j} \right] + (1 - F_1) \frac{2\rho}{\sigma_{\omega,2}} \frac{1}{\omega} \frac{\partial k}{\partial x_j} \frac{\partial \omega}{\partial x_j} \quad (2)$$

The transport equations of the SAS-SST model (1) and (2) differ from those of the SST RANS model by the additional SAS source term Q_{SAS} in the transport equation for the turbulence eddy frequency ω , (2). In (2) $\sigma_{\omega,2}$ is the σ_ω value for the k - ϵ regime of the SST model.

The meaning of the additional source term Q_{SAS} is according the relation:

$$Q_{SAS} = \max \left[\rho \eta_2 k S^2 \left(\frac{L}{L_{vk}} \right)^2 - C \frac{2\rho k}{\sigma_\omega} \max \left(\frac{1}{\omega^2} \frac{\partial}{\partial x_j} \frac{\partial}{\partial x_j} \frac{1}{k^2} \frac{\partial k}{\partial x_j} \frac{\partial k}{\partial x_j} \right), 0 \right] \quad (3)$$

This SAS source term originates from a second order derivate term in Rotta’s transport equations. The model parameters in the SAS source term (3) are: $\eta_2 = 3,51$; $\sigma_\omega = \frac{2}{3}$; $C = 2$.

Here L is the length scale of the modeled turbulence:

$$L = \frac{\sqrt{k}}{\left(c_\mu^{1/4} \omega \right)}, \quad (4)$$

and the von Karmen length scale L_{vk} is a three-dimensional generalization of the classic boundary layer definition $L_{vk}^{2D} = k \frac{\partial u}{\partial y} / \left(\frac{\partial^2 u}{\partial y^2} \right)$.

$$L_{vk} = \frac{kS}{|U^m|} \quad (5)$$

The first velocity derivative $\frac{\partial u}{\partial y}$ is represented in L_{vk} by S, which is a scalar invariant of the rate tensor S_{ij} :

$$S = \sqrt{2S_{ij}S_{ij}}, S_{ij} = \frac{1}{2} \left[\frac{\partial u_i}{\partial x_j} + \frac{\partial u_j}{\partial x_i} \right] \quad (6)$$

Note, that the same S also directly participates in Q_{SAS} (3) and in the turbulence production term $P_k = \mu_t S^2$. The second velocity derivative $|U''|$ is generalized to 3D using the magnitude of the velocity Laplacian:

$$|U''| = \sqrt{\sum_{(i,j)} \left(\frac{\partial^2 u_i}{\partial x_j \partial x_j} \right)^2} \quad (7)$$

So defined L and L_{vk} are both equal to (ky) in the logarithmic part of the boundary layer, where $k=0,41$ is the von Karmen constant.

The model also provides a direct control of the high wave number damping. This is realized by lower constrain on the L_{vk} value in the following way:

$$L_{vk} = \max \left(\frac{kS}{|U''|}, C_S \sqrt{\frac{k\eta_2}{(b/c_\mu) - \alpha}} \Delta \right), \Delta = \Omega_{CV}^{1/3} \quad (8)$$

This limiter is proportional to the grid size Δ , which is calculated as the cubic root of the control volume size Ω_{CV} . The purpose of this limiter is to control damping of the finest resolved turbulent fluctuations. The structure of the limiter is derived from analyzing the equilibrium eddy viscosity of the SAS-SST model.

RESULTS. DISCUSSIONS

The numerical study was performed for a flow passed over square cylinder. The results were compared with the experimental data provided by [5]. The experiment is conducted in a water tunnel with 0,56m x 0,39m test section. The square cylinder is 0,04m x 0,04m (7% blockage ration) with 0,39m in length, and free stream flow speed is 0,535 m/s with 2% turbulence intensity. A SAS simulation was conducted for the configuration of the experiment. The computational domain is 20D x 14D x 2D with 104 x 69 x 10 grid points in the streetwise, the lateral, and the axial direction, respectively. In the present study, simulation is carried out in two dimensions. The governing equations solved are the conservation of mass and momentum.

During the process of numerical modeling a couple of different input data have been tested. The different regimes are presented in table 3.

Input data

Table 3. Input data for the CFD tool

No	Model	Velocity Magnitude (m/s)	Turbulent Intensity %	Turbulent Length Scale (m)	Scheme	Gradient	Pressure	Momentum	Turbulent Kinetic Energy	Specific Dissipation Rate	Transient Formulation
1	SAS	0.535	2	0.0028	SIMPLE	Green-Gauss Cell Based	Second Order	Bounded Central Differencing	Second Order Upwind	Second Order Upwind	Second Order Implicit
2	SAS	0.535	2	0.0028	SIMPLE	Green-Gauss Node Based	Second Order	Bounded Central Differencing	Second Order Upwind	Second Order Upwind	Second Order Implicit
3	SAS	0.535	2	0.0028	SIMPLE	Least Squares Cell Based	Second Order	Bounded Central Differencing	Second Order Upwind	Second Order Upwind	Second Order Implicit
4	SAS	0.535	2	0.004	SIMPLE	Green-Gauss Node Based	Second Order	Bounded Central Differencing	Second Order Upwind	Second Order Upwind	Second Order Implicit
5	SAS	0.535	2	0.01	SIMPLE	Green-Gauss Node Based	Second Order	Bounded Central Differencing	Second Order Upwind	Second Order Upwind	Second Order Implicit
6	SAS	0.535	2	0.19	SIMPLE	Green-Gauss Node Based	Second Order	Bounded Central Differencing	Second Order Upwind	Second Order Upwind	Second Order Implicit
7	SAS	0.535	2	0.028	SIMPLE	Green-Gauss Node Based	Second Order	Bounded Central Differencing	Second Order Upwind	Second Order Upwind	Second Order Implicit
8	SAS	0.535	2	0.028	PISO	Green-Gauss Node Based	Second Order	Bounded Central Differencing	Second Order Upwind	Second Order Upwind	Second Order Implicit

Numerical solution results

On the figures below are presented the results from the numerical solution in accordance with the previously accepted initial conditions. The contours in the figures represent the velocity and turbulent energy distribution behind the submerged square cylinder. Concerning the accepted SAS turbulent model the large-scale eddies are

calculated while small-scale eddies are modeled. On Figure 3 are presented the results from numerical solution using different schemes for calculation the gradient – Green – Gauss and Least squares cell based. It is obvious that the velocity contours after the body are close while a big difference in turbulent kinetic energy is observed.

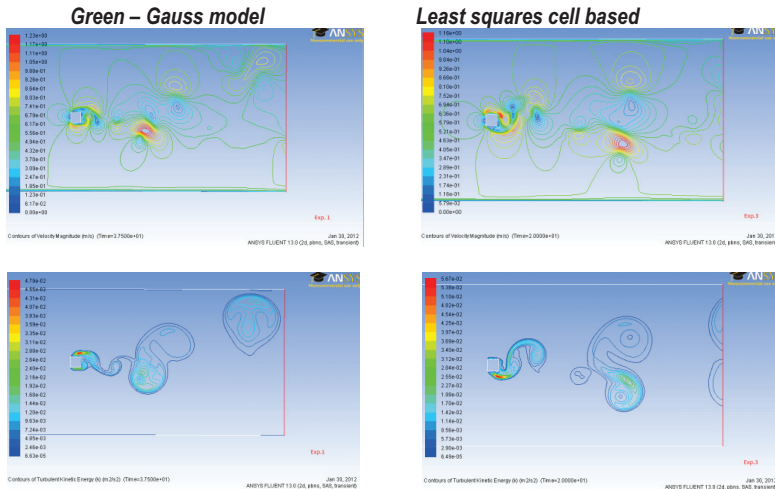


Figure 3. Contours of velocity and turbulent kinetic energy past square-cylinder (approaches for gradient calculation)

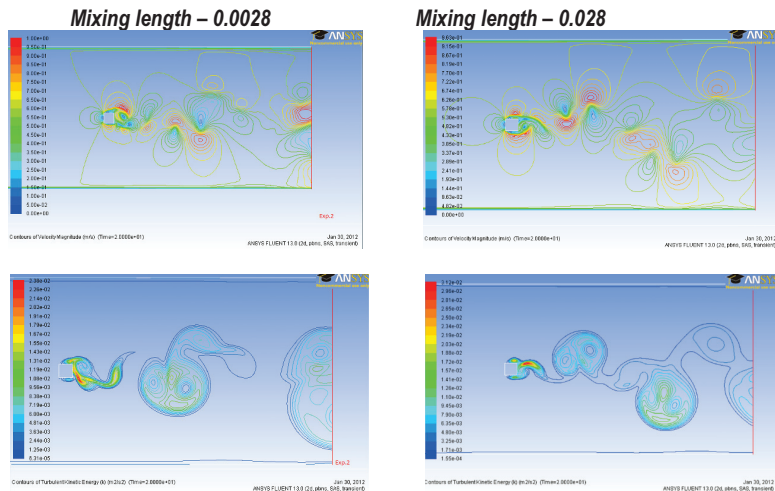


Figure 4. Contours of velocity and turbulent kinetic energy past square-cylinder (mixing length approaches)

On the figure 4 are presented the same contours of constant velocity and turbulent energy using different mixing lengths in input data. Figures 3 and 4 show that velocity profiles using “Least squares cell based” and “Mixing length” in a certain regions are most similar. The turbulent kinetic energy distribution in all cases differs and only adjustments to

the model based can be made based on the experimental data.

CONCLUSION

In the paper was presented an overview of the recently developed and used turbulent models in modeling of unsteady flow past submerged bodies. Different turbulent models have been proposed and tested as the results were compared with the available in the literature experimental data. The better comparison between numerical and experimental results is observed when using the SAS-SST model that adjusts already resolved scales in a dynamic way and allows the development of a turbulent spectrum in the detached regions. Also improvement in the numerical results are observed using “Green – Gauss model” and a greater mixing length in the amount of 0.028.

BIBLIOGRAPHY

- [1] Wang, Q., K. D. Squires, Large-eddy simulation of particle-laden turbulent channel flows, *Phys. Fluid* 8, 1207 – 1223, 1996;
- [2] Okajima A., Strouhal number of rectangular cylinder, *J. Fluid Mech.* 123, 379 – 398, 1982;
- [3] Okajima A., Numerical analysis of the flow around an oscillating cylinder, In P. W. Bearman (Ed.), *Proc. 6th Int. Conference flow-induced vibration*, London, UK, 10-12 April, p.p. 1-7, Balkema, Rotterdam, 1995.
- [4] Duraõ D. F. G., M. Heitor, J. Pereira, Measurements of turbulent and periodic flows around a square-section cylinder, *Exps. Fluids* 6, 298 – 304, 1988.
- [5] Lyn D. A., S. Einav, W. Rodi, J. H. Park, A laser-Doppler velocimetry study of ensemble-averaged characteristics of the turbulent near wake of a square cylinder, *Journal of Fluid Mechanics*, Vol. 304, December 1995, p.p. 285 – 319.
- [6] Rotta J.C., *Turbulence strömungen*, 267, S.m. 104, Fig. Stuttgart 1972, B. G. Teubner, Preis, geb. – DM (pages 129 – 130).

Contact:

Assoc. Prof. Angel Terziev, Ph.D., Dept. “Hydroaerodynamic and hydraulic machines”, Technical University of Sofia, phone + 359 (02) 965 3443, e-mail: aterziev@tu-sofia.bg

The paper is reviewed